

# Geometry-related Treatments for Three-dimensional Meshless Method

Ming-Hsiao Lee<sup>1,2</sup> and Wen-Hwa Chen<sup>1,3</sup>

**Abstract:** The meshless method has a distinct advantage over other methods in that it requires only nodes without an element mesh which usually induces time-consuming work and inaccuracy when the elements are distorted during the analysis process. However, the element mesh can provide more geometry information for numerical simulation, without the need to judge if the nodes or quadrature points are inside the analysis domain which happens in the meshless method, since the analysis domain is defined by the element's edges or faces and the quadrature points are all inside the elements. Because the analysis model with only nodes for the meshless method lacks these types of geometry-related information, some difficulties are usually encountered during the numerical simulation, especially, for the cases with three-dimensional irregular-shaped analysis domains. Therefore, two types of domain and boundary representations, say, constructive solid geometry scheme and triangulated surface boundary scheme, are employed in this work. To further deal with those geometry-related issues required for the meshless method, several efficient check mechanisms are also devised. With those proposed geometry schemes and check mechanisms, both three-dimensional irregular-shaped and multi-material problems can be easily handled with the meshless method. Several demonstrative cases prove the effectiveness of the proposed techniques.

**Keywords:** meshless, geometry treatment, triangulated surface, multi-material

## 1 Introduction

One of the main disadvantages of the finite element method is that it requires a mesh, including elements and nodes, which is usually time-consuming for preparation and sometimes induces inaccuracy when the elements are distorted in dealing

---

<sup>1</sup> Dept. of Power Mech. Engng., National Tsing Hua University, Hsinchu, Taiwan, ROC

<sup>2</sup> National Center for High-performance Computing, National Applied Research Laboratories, Taiwan, ROC

<sup>3</sup> National Applied Research Laboratories, Taiwan, ROC

with engineering problems. On the contrary, the meshless method has an inherent advantage that it does not require any mesh and uses only nodes. This method has become one of the most promising numerical methods. Based on similar ideas, there have been emerging various meshless methods, such as, the element-free Galerkin method (EFGM)[Belytschko, Lu, and Gu (1994)], the reproducing kernel particle method [Liu, Jun, and Zhang (1995)], the  $h - p$  clouds [Duarte and Oden (1996)], the meshless local Petrov-Galerkin method [Atluri and Zhu (1998)], the node-by-node meshless method [Nagashima (2000)], etc. Although there were pioneering successes by those works, most of them were limited to two-dimensional problems. Till recent years, three-dimensional problems, but only with simple geometry, have then been tackled [Chen and Guo (2001); Li, Shen, Han and Atluri (2003); Han and Atluri (2004); Chen and Chen (2005); Chen, Chi, and Lee (2009)]. Part of the reason is due to the difficulty to deal with irregular domains in three-dimensional realistic engineering problems.

Although the meshless method does not need an element mesh and can avoid the disadvantages of the mesh, however, the element mesh provides some useful geometry information required for numerical simulation, for example, the boundaries of the analysis domain are represented by the element's edges or faces and the integration points of elements are all located inside the analysis domain. Because the meshless analysis model lacks these types of geometry-related information, some extra treatments should be performed during numerical simulation. In the practical implements of meshless method, for examples, the element free Galerkin method, an efficient procedure can be stated as follows:

- (1) Generate node data:
  - a. Distribute the nodes regularly in the space, which should be big enough to cover the entire analysis domain.
  - b. Exclude those nodes outside the boundaries of the analysis domain.
- (2) Generate the regular background cells to cover the entire analysis domain and its boundaries for numerical integration.
- (3) Form the stiffness matrix:
  - a. Take integration over cells by quadrature.
  - b. Check if any quadrature point in cell outside the analysis domain. If yes, ignore that quadrature point.
  - c. Choose appropriate surrounding nodes to define the sub-domain for the quadrature point which is inside the analysis domain.

- d. Determine if any surrounding nodes blocked by the boundary segment. If yes, exclude that node from the sub-domain.
  - e. Calculate the shape functions for the quadrature point by the moving least squares method.
  - f. Evaluate the stiffness matrix assembled from all the quadrature points.
- (4) Apply the loadings and boundary conditions.
- (5) Solve the final simultaneous equations.

As stated above, one needs to determine if any nodes or the quadrature points outside the boundaries of the analysis domain as mentioned in steps (1)-b. and (3)-b. Besides, one also needs to determine if any surrounding nodes of the quadrature point blocked by any boundary segment as indicated in step (3)-d. To solve these, accurate geometry representations for the analysis domains and their boundaries and efficient check mechanisms are imperative. In the cases of three-dimensional problems with irregular-shaped analysis domains, unfortunately, such treatments cannot be done by the analysis model with only node data.

To overcome the difficulties, two geometry schemes which have been widely used in CAD/CAM tools [Zeid (1991)] are employed in this work. For regular analysis domains, the constructive solid geometry scheme that forms geometric shapes using a number of basic primitives and appropriate set operations is adopted due to the advantage of simplicity and easy manipulation. But, it has its limitation to deal with irregular-shaped analysis domains. Therefore, for three-dimensional irregular-shaped analysis domains, the triangulated surface boundary scheme [Atluri, Han and Rajendran (2004)] is chosen here. By this scheme, the surfaces of the three-dimensional analysis domain are formed with triangular facets and can be easily built by auto-mesh generators whenever the geometry data is available. In addition to the geometry schemes, several check mechanisms are also required and proposed in this work. By those proposed geometry schemes and check mechanisms, the difficult geometry-related treatments can be handled even for the three-dimensional irregular-shaped analysis domains with complicated concave boundaries or internal holes.

Similarly, in cases comprising multiple materials in three-dimensional analysis models, the irregular-shaped interfaces between different materials can cause the same problems as encountered with general surface boundaries. The proposed geometry schemes and check mechanisms can be further applied to solve such problems. With the techniques developed in this study, the interfaces between different materials in these cases can also be treated as the boundaries and defined by the

triangulated surface boundary scheme. The necessary checks as mentioned above are then performed accordingly.

Three simulation examples have been solved to validate the proposed schemes and check mechanisms. The first one is a comb-drive with regular analysis domain and solved with the constructive solid geometry scheme. Another one is a silicon microphone with complicated analysis domain and solved with the triangulated surface boundary scheme. The last one is the middle ear ossicles of guinea pigs, containing irregular shape and multiple materials, and also solved with the triangulated surface boundary scheme.

## **2 Define analysis domain and its boundaries**

In the finite element method, the elements themselves provide enough geometry information of analysis domain and its boundaries, no matter for two-dimensional or three-dimensional cases. But, it is not the case in the meshless method. Therefore, it is imperative to find some way to adequately and efficiently define the analysis domain and its boundaries. In two-dimensional analysis domain, the boundaries are easy to define just by connecting the boundary nodes with straight lines. Nevertheless, in three-dimensional problems, the geometry becomes more complicated, especially for those with irregular sculptural faces. Here, the constructive solid geometry scheme and the triangulated surface boundary scheme are adopted for three-dimensional problems. The constructive solid geometry scheme is for regular-shaped analysis domains, and the triangulated surface boundary scheme is for irregular-shaped analysis domains.

### **2.1 Constructive solid geometry schemes**

The constructive solid geometry scheme is a popular schemes used to define and create geometry models in CAD. In this scheme, the geometry model is constructed by combining various types of primitives, say, block, sphere and cylinder, etc., with some set operations, such as union, intersection and subtraction. This scheme is simple and easy to employ in defining the analysis domain for the meshless method. Although it has limitation, such as difficulty in creating irregular geometry which cannot be modeled with those basic primitives by using set operations, it still can be used efficiently for many cases due to its simplicity, which can save a substantial amount of computing time.

Typical primitives used in this scheme are blocks, spheres and cylinders, as shown in Fig. 1(a). There is no problem determining the territory of those primitives. They can be represented by a set of coordinate ranges or mathematical expressions. For example [Zeid (1991)],

$$\text{Block } (L \times W \times H) \quad \{(x, y, z) : 0 \leq x \leq L, 0 \leq y \leq W, \text{ and } 0 \leq z \leq H\} \quad (2.1)$$

$$\text{Cylinder } (r \times H) \quad \{(x, y, z) : x^2 + y^2 \leq r^2, \text{ and } 0 \leq z \leq H\} \quad (2.2)$$

$$\text{Sphere } (r) \quad \{(x, y, z) : x^2 + y^2 + z^2 \leq r^2\} \quad (2.3)$$

These basic shapes can be combined to represent some more complicated analysis domains by using set operations. As shown in Fig 1, after set operations, the analysis domain is combined with two different blocks, a cylinder and a sphere. Unify the two blocks first, and subtract the cylinder and sphere from it. These operations can easily be programmed into the meshless codes without consuming much computing time.

This scheme provides an easy and efficient way to handle the definition of regular-shaped analysis domains for the meshless method. For example, judging if a point falls within the analysis domain can simply be done by checking whether that point is within the set of the model.

## 2.2 *Triangulated surface boundary scheme*

For three-dimensional problems, the triangulated surface boundary scheme is proposed to represent the surfaces of the three-dimensional analysis domain with triangular facets [Atluri, Han and Rajendran (2004)] which can be generated by most CAD tools or pre-processors. This type of geometry format, also known as stereo lithography (STL) format, has been widely used in the applications for rapid prototyping, computer-aided manufacturing, and computer graphics. It becomes a basic way to represent three-dimensional irregular geometry.

Triangular facets are not triangular elements, such as those used in the finite element method. They are utilized only for geometry treatment purposes. As shown in Fig. 2, the complicated and irregular geometry of the ossicles of the middle ear of a guinea pig is represented by the triangulated surface boundary scheme. There also are 11,132 nodes automatically paved to cover the ossicles by the program, as mentioned in step (1)-a in section 1, for later use.

## 3 Check mechanisms

In addition to the information of analysis domain and boundaries, there are various types of geometry-related treatments needed for the meshless method. For examples, one needs to determine if certain points are located inside the analysis domain, or to determine if the node is inside the sub-domain for forming the moving least-squares interpolant. Several efficient check mechanisms are proposed herein.

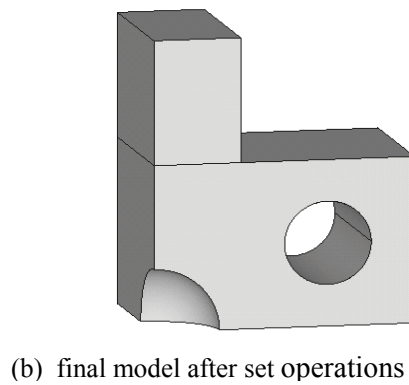
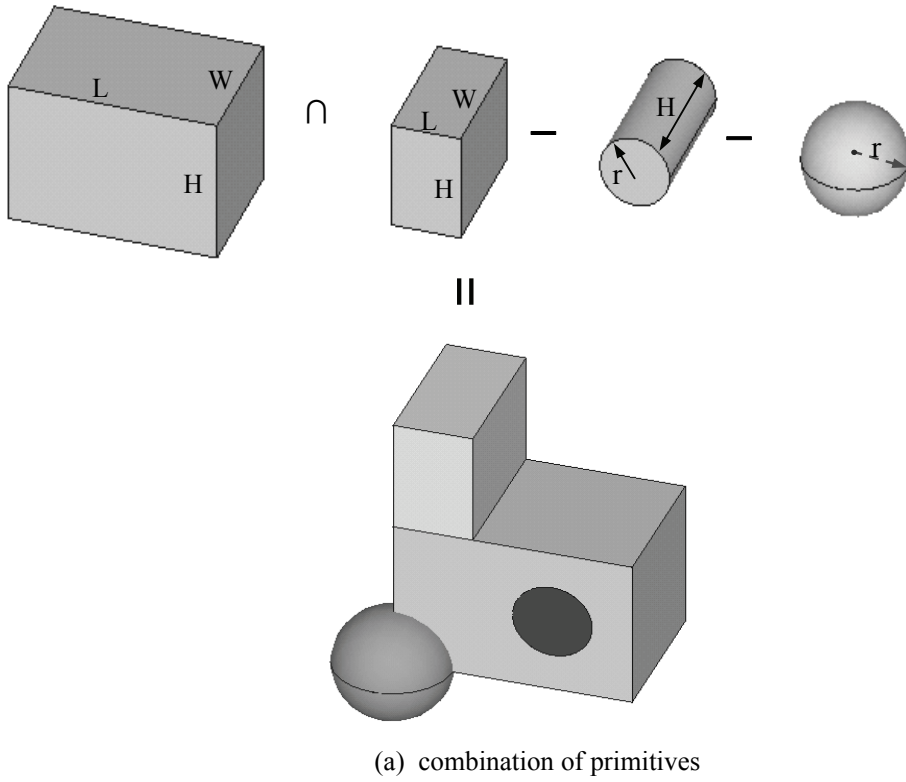


Figure 1: The analysis domain represented by constructive solid geometry scheme with set operations

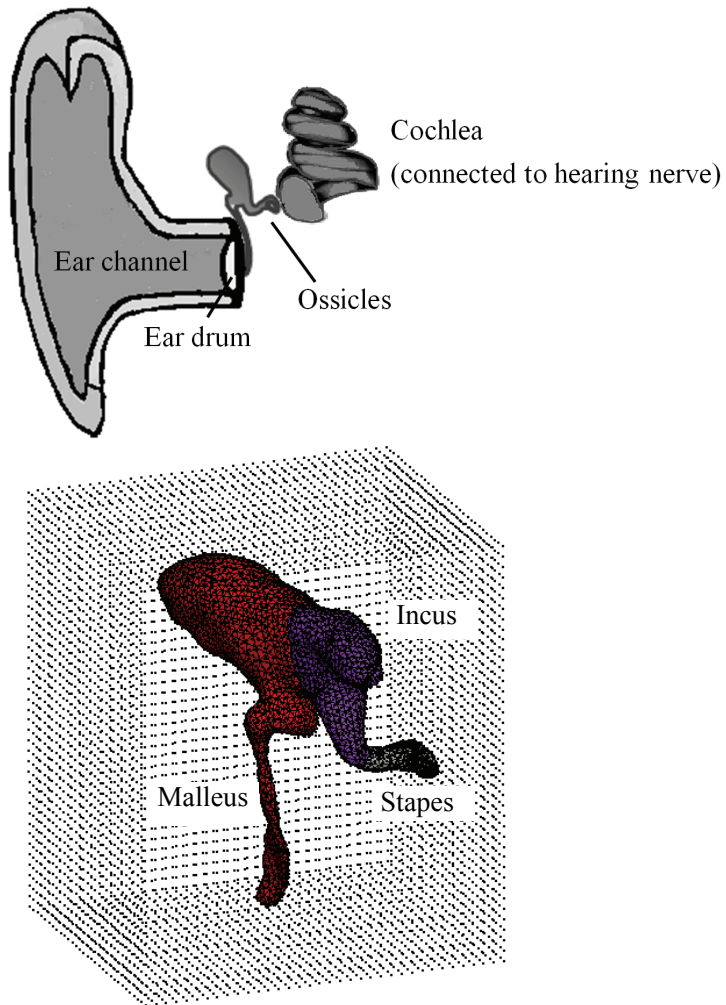


Figure 2: Guinea pig's ossicles represented by triangulated surface boundary scheme

### 3.1 Determine inside or outside the analysis domain

In the meshless method, as stated in steps (1)-b and (3)-b in section 1, there are several occasions in which it is necessary to determine if any nodes or quadrature points are inside or outside the analysis domain. It is worthwhile to mention that when a background grid scheme [Chen, Chi, and Lee (2009)] is used to solve extremely large deformation problems, program also needs to determine whether the nodes of the background grid fall inside or outside the continually deformed analysis domains.

When the constructive solid geometry scheme is employed to define a regular-shaped analysis domain, judging whether a node or a quadrature point is inside the analysis domain can be done simply by checking if the node or quadrature point is in the set of the model as described in section 2.1.

As the boundaries of the analysis domain are represented by the triangulated surface boundary scheme, a different check mechanism is required to handle those geometry-related operations. For the sake of clarity, a two-dimensional description is drawn as shown in Fig. 3. First, a reference point is selected inside the analysis domain. The internal reference point must be assured to lie within the domain. This needs to be done automatically in the meshless program. After the internal reference point has been created properly, when one wants to check if a discussed point lies within the analysis domain, just connect the discussed point to the internal reference point with a connecting line. Next, check whether the connecting line crosses any boundaries of the analysis domain. Even when a connecting line has crossed the boundaries, the discussed point might still be in the analysis domain. When the connecting line crosses the boundaries an odd number of times, it is concluded that the discussed point lies outside the analysis domain; otherwise, the discussed point is inside the analysis domain. By this mechanism, one can effectively determine if the discussed node or quadrature point is inside the analysis domain, even if there are internal holes or complicated concave boundaries contained within the three-dimensional irregular-shaped analysis domain.

Alternatively, one can create a reference point located outside the analysis domain. Identifying a point to be outside the analysis domain is easier than for those inside. First, as shown in Fig. 4, one defines a bounding box big enough to cover the entire analysis domain by selecting the minimum and maximum coordinates of all the boundary nodes in the analysis model. Next, create an external reference point outside the bounding box and connect it to the discussed point with a connecting line. By following a procedure similar to the one mentioned earlier with the internal reference point, one can check if the connecting line crosses any boundary facets, as shown in Fig. 5. In this case, the criterion is opposite to that with the internal

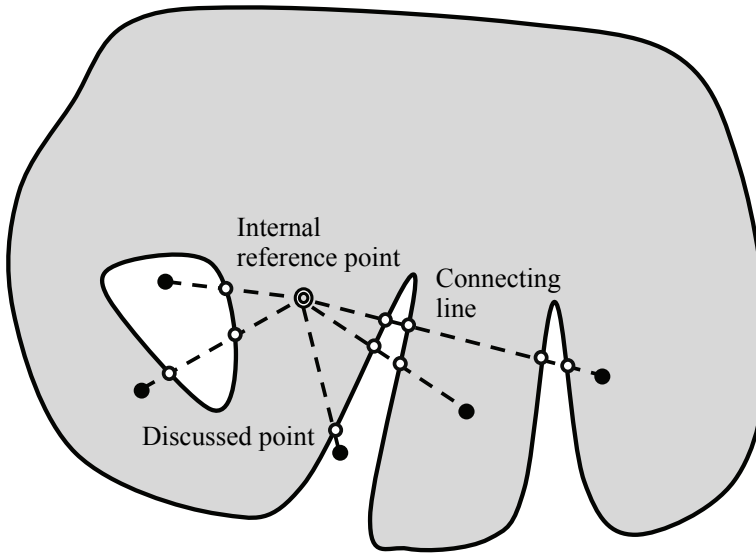


Figure 3: Determine inside or outside the analysis domain with an internal reference point

reference point. In other words, if the connecting line crosses the boundaries an odd number of times, the discussed point lies within the analysis domain; otherwise, the point is outside the analysis domain.

It is obvious that the external reference point is easier to choose. But for the internal reference point case, one can compute its shortest distance to the boundaries in the beginning of the analysis process. As the length of the connecting line is shorter than that distance, one can directly pass those discussed points without having to check further. This can save computing time.

If a connecting line crosses the surface boundaries of a three-dimensional analysis domain, certain triangular facet will be intersected by that connecting line. It means that, when one wants to know how many times a connecting line crosses the surface boundaries, this can be determined by checking how many triangular facets have been pierced by that connecting line. As shown in Fig. 6., for three-dimensional representation, a connecting line intersects the plane on which the triangular facet in question lies at point  $x$ . If the line intersects the triangular facet, point  $x$  should fall within the facet; otherwise, the line does not intersect the facet. To determine this, first, compute the normal distance from point  $P$  to point  $R$  on the plane and the component of  $\vec{PQ}$  on the normal  $\vec{PR}$ , i.e.  $\vec{PS}$ .  $\xi$  is the length ratio of  $\vec{PR}$  to  $\vec{PS}$ . One can then determine the coordinates of the intersection point  $x$ ,  $u(x)$ , with those of

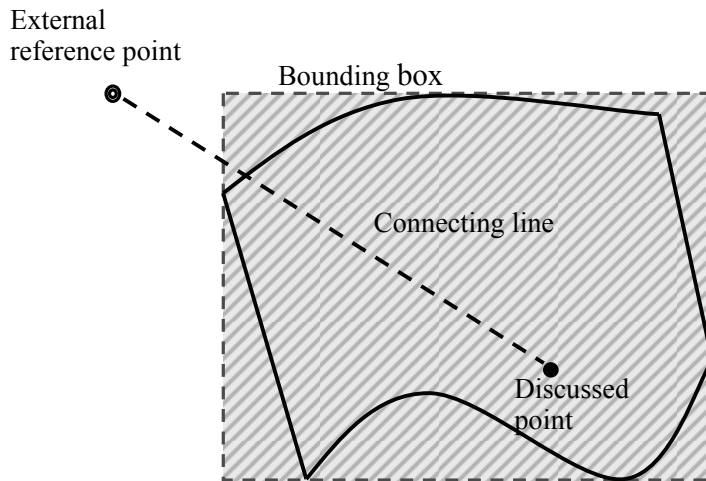


Figure 4: The check mechanism with an external reference point

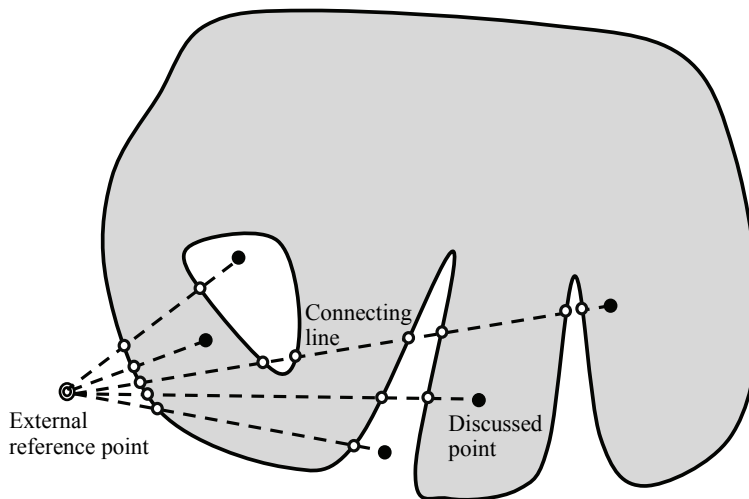


Figure 5: Determine inside or outside the analysis domain with an external reference point

point P and Q,  $u(P)$  and  $u(Q)$ , by linear interpolation:

$$u(x) = (1 - \xi)u(P) + \xi u(Q). \quad (3.1)$$

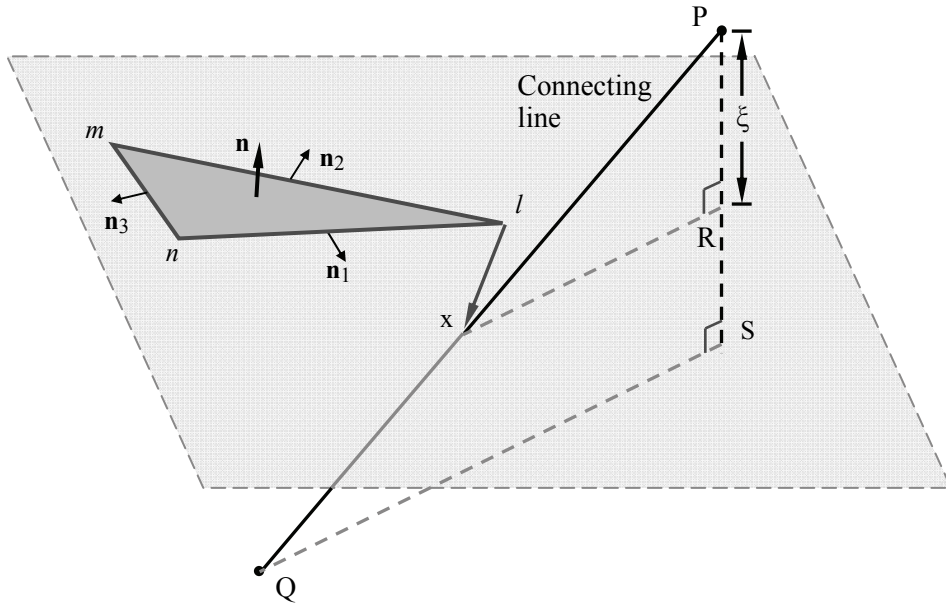


Figure 6: Check if the connecting line intersects the discussed triangular facet

As illustrated in Fig. 6, there are three outward normal vectors to the three edges of that facet, namely  $\mathbf{n}_1$ ,  $\mathbf{n}_2$  and  $\mathbf{n}_3$ . To determine if point  $x$  is inside an edge, connect a vertex of the discussed edge and point  $x$  to form a vector, e.g.  $\vec{l x}$  and take a scalar product between vector  $\vec{l x}$  and the normal vector to that edge, e.g.  $\mathbf{n}_1$ . If the result is negative, point  $x$  is inside that edge. If point  $x$  is inside all three edges, it means that the point  $x$  is inside that facet and the connecting line has intersected that facet.

### 3.2 Determine sub-domain

Another common need for the meshless method is to form the sub-domain for calculating the moving least-squares interpolant. As one encircles all the nodes located inside the influence radius of a quadrature point, it is necessary to determine if any of those nodes are blocked by a boundary segment in-between; if so, that node should be excluded from the sub-domain, as mentioned in the meshless simulation procedure step (3)-d. To do this, a similar check mechanism is shown in Fig. 7.

As the quadrature point and the discussed node are connected with a connecting line, if the connecting line crosses any boundary, the two points are blocked by

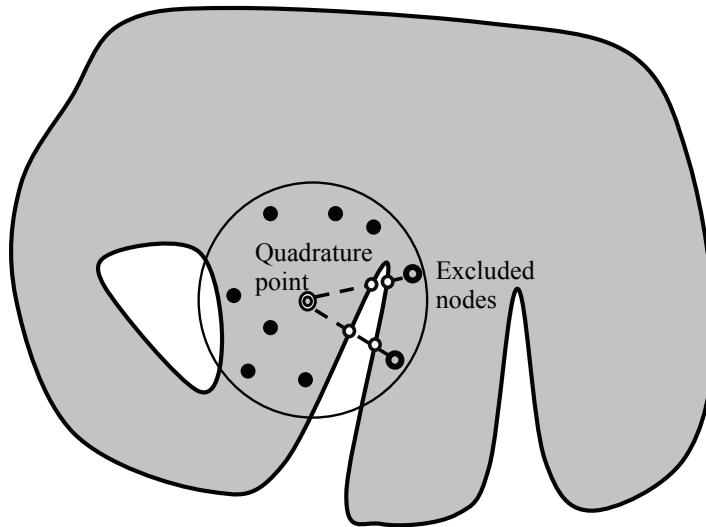


Figure 7: Determine sub-domain

that boundary. One can infer that the two points are invisible to each other and the discussed node should be excluded from the sub-domain.

For the constructive solid geometry scheme, there is a variety types of surfaces to be handled. For blocks, the boundary surfaces are rectangular. For cylinders, the surfaces are circular and cylindrical. For spheres, their surfaces are spherical. For each type of surfaces, similar check mechanism is utilized. The operations to check whether the connecting line crosses the surfaces are as follows:

The rectangular surfaces of blocks are similar to triangular facets except that they include an additional edge. Therefore, the operation to check them is similar to that with the triangular facet, as seen in Fig. 6, except checking one additional edge.

For spherical surfaces, one needs to determine the point on the connecting line with the shortest distance to the sphere's center and compare the distance to the sphere's radius  $r$  as shown in Fig. 8 to see if the connecting line crosses the sphere's face.

First, connect one end of the connecting line  $\vec{PQ}$  and the sphere's center to form a vector  $\vec{PO}$ . Next, take the scalar product of the vector  $\vec{PO}$  and the unit vector along  $\vec{PQ}$ . The component of the vector  $\vec{PO}$  on the vector  $\vec{PQ}$  can determine the point  $x$  which is the closest point to the sphere's center. The distance  $r_1$  can then be calculated. If  $r_1$  is longer than the radius of sphere  $r$ , the connecting line does not cross the spherical face. If  $r_1$  is shorter than the radius of sphere  $r$ , one needs to check if the points  $P$  and  $Q$  are inside the sphere. If both are inside, there is no

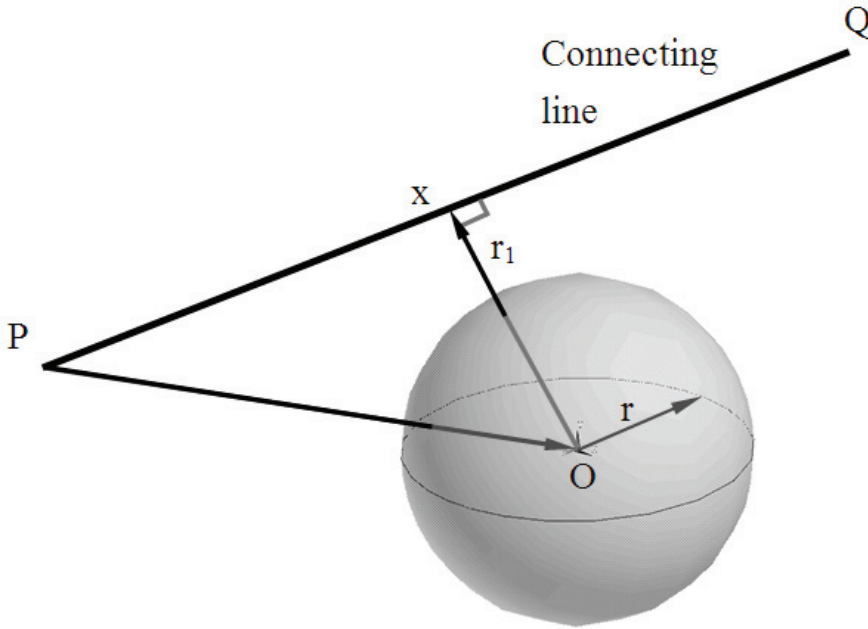


Figure 8: Check if the connecting line crosses spherical primitive’s face

intersection. If one is inside and the other is outside, the connecting line does cross the sphere’s face and the discussed node should be excluded. If both are outside, one needs to check if the points P and Q are located on different side of the sphere by doing scalar products of the vector  $\vec{OP}$  or  $\vec{OQ}$  with the vector  $\vec{PQ}$ . If the signs of the products are different, it means that the connecting line indeed crosses the sphere’s face.

For the surfaces of cylinders, one needs to determine the shortest distance between the connecting line  $\vec{PQ}$  and the axis line of the cylinder, i.e.  $\vec{O_1O_2}$  as shown in Fig. 9, and compare the distance  $r_1$  to the cylinder’s radius  $r$  to know if the connecting line crosses the cylinder’s face. The way to determine the shortest distance between the two lines is: [Johnson, Kiokemeister, and Wolk (1978)]

$$\vec{w} = \vec{PQ} \times \vec{O_1O_2} \tag{3.2}$$

$$r_1 = |\vec{PO_1} - \vec{w}| / |\vec{w}| \tag{3.3}$$

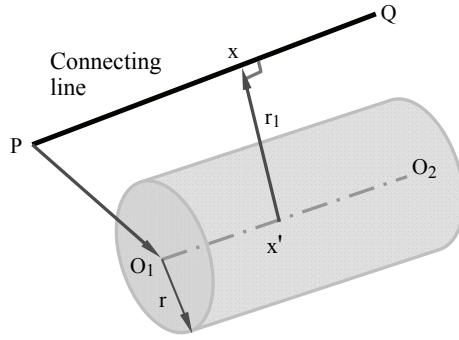
If  $r_1 > r$ , as shown in Fig. 9 (a), the connecting line does not cross cylinder’s faces. If  $r_1 < r$ , further checking is needed. First, determine both the closest points, P’ and

$Q'$ , on axis line  $\overrightarrow{O_1O_2}$  to the vertex point  $P$  and  $Q$ . If  $P'$  and  $Q'$  are both inside the cylinder, the connecting line has crossed the cylinder's face as shown in Fig. 9 (b), except the case that both point  $P$  and  $Q$  are inside the cylinder, i.e. the distances of vector  $\overrightarrow{PP'}$  and  $\overrightarrow{QQ'}$  are shorter than the radius of the cylinder  $r$ . If more than one of  $P'$  or  $Q'$  is outside the cylinder, one needs to determine the intersection point on the cylinder's end face and check the distance between the intersection point and the center of the end face, i.e.  $r_2$ , as shown in Fig. 9 (c). If  $r_2 < r$ , the connecting line does cross cylinder's faces. Otherwise, there is no intersection. When intersection happens, the discussed node should be excluded.

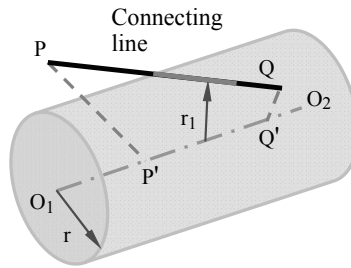
When employing the triangulated surface boundary scheme for three-dimensional irregular-shaped problems, one uses a similar way to determine the sub-domain as shown in Fig. 6 and Fig. 7. If the connecting line between the quadrature point and the discussed node crosses any triangular facet, there is definitely a boundary segment in-between the points, and the discussed node should be excluded from the sub-domain.

#### 4 Treatments of multi-materials

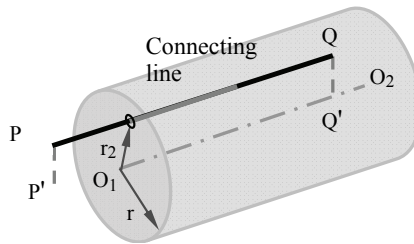
In the case where the analysis domain includes more than one material, since the material properties in different portions of the analysis domain are not the same, the weak form integrals of the equilibrium equations of different materials need to be obtained separately. In general, the sub-domain of the quadrature point for the moving least squares interpolant can not cross the material interface due to the discontinuity of the material properties. In this situation, the interfaces between two adjacent materials can be considered another type of boundary. Similarly, three-dimensional irregular-shaped interfaces between different materials will cause the same difficulties for the meshless method as those that occurred with general surface boundaries during the analysis steps, such as checking if the quadrature point or node lies within a particular material or checking if any nodes of the sub-domain should be excluded when they are blocked by certain interface segment. Therefore, to deal with these, effective geometry representations for the interfaces and efficient check mechanisms are again required. Hence, the proposed geometry schemes and check mechanisms for the general boundaries of the analysis domain as mentioned above can also be employed here. Especially, when dealing with irregular-shaped interfaces, the triangulated surface boundary scheme can again be used to define the interfaces. In practical implements, different materials will have their own boundary surfaces, but, they share the same interface surfaces between two adjacent materials which will be triangulated as done to general boundaries. Besides, those nodes of two different materials located on the interfaces between two materials need to be the same ones or connected by multiple point constraints (MPC).



(a)  $r_1 > r$



(b)  $r_1 < r$ , P' and Q' inside the cylinder



(c)  $r_1 < r$ , P' or Q' not inside the cylinder

Figure 9: Check if the connecting line crosses cylindrical primitive's faces

One can just create one triangulated surface for one material and shares it with the adjacent material.

When calculating the weak form integrals of the equilibrium equations during the normal procedure of the meshless method, the numerical integration is carried out separately for each material. When performing the inside/outside checks, the check mechanism is the same as described above, just as each material has its own boundaries including the interfaces. In addition, the sub-domain for each quadrature point in a particular material must also not cross the interfaces which can be achieved by the proposed check mechanism. Because they have shared the same nodes on the interfaces among adjacent materials, the numerical integrals of the weak form of the equilibrium equations for the whole structure, such as stiffness matrix, will be assembled and formed automatically.

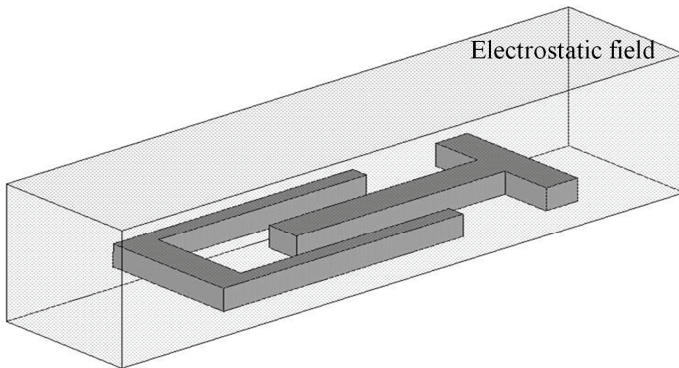
## 5 Results and discussion

In this study, three numerical examples were carried out to validate and demonstrate the effectiveness of the proposed geometry schemes and check mechanisms. Without loss of generality, the meshless method employed here was based on the element-free Galerkin method. For comparison purposes, the finite element solutions calculated by ANSYS program for the same problems were also presented.

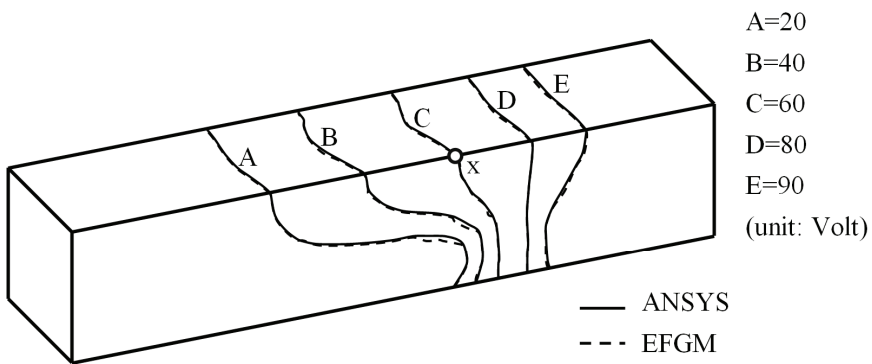
The first example was a pair of electrostatic-driven comb-drive fingers as shown in Fig. 10(a). An electrostatic analysis was conducted. A charge of zero voltage was applied to the left electrode and a charge of 100 volts was applied to the right electrode. A moderate size of free space was adopted for electrostatic field analysis. The length, width, and thickness of the fingers are  $20\mu\text{m}$ ,  $3\mu\text{m}$ , and  $2\mu\text{m}$ , respectively. The gap between fingers is  $3\mu\text{m}$ . The overlap between fingers is  $12\mu\text{m}$ . The shape of the analysis domain is a regular three-dimensional geometry. To solve this example, the constructive solid geometry scheme was employed. The results of electric potential distribution are shown in Fig. 10(b). A convergence study was conducted using 10-node quadratic elements by ANSYS program. As listed in Table 1, the computed electric potentials at point x, as seen in Fig. 10(b), converged to 60.0 Volts as compared with 58.8 Volts by the element-free Galerkin method with 2% difference. Excellent agreement of the computed electrical potential distributions between the element-free Galerkin method and ANSYS program is drawn.

The second example is the analysis of a silicon microphone. In a silicon microphone, a diaphragm and a perforated backplate form a pair of capacitor, which performs as a transducer to convert sound wave into electrical signals. The sound pressure will induce the deflection of the diaphragm and change the gap between

the diaphragm and the backplate. The capacitance of the capacitor, which is a manipulable electrical signal, is then changed accordingly. To evaluate the acoustic characteristics of the silicon microphone, as shown in Fig. 11(a), an electrostatic analysis has been conducted. The radius of the backplate and diaphragm is  $180\ \mu\text{m}$ .



(a) constructive solid geometry scheme for comb-drive fingers



(b) electric scalar potential distribution

Figure 10: Electrostatic analysis of a comb drive

The thicknesses of the backplate and diaphragm are  $2\ \mu\text{m}$  and  $0.4\ \mu\text{m}$ , respectively. The radius of the ventilation holes on the backplate is  $5\ \mu\text{m}$ . The gap between

Table 1: Comparison of the computed electric potentials at point x

Method	No. of elements	No. of nodes	Electric potential (Volt)
ANSYS	5,005	2,947	58.1
	5,706	3,394	59.8
	7,555	4,578	59.9
	12,651	7,994	60.0
EFGM		4,868	58.8

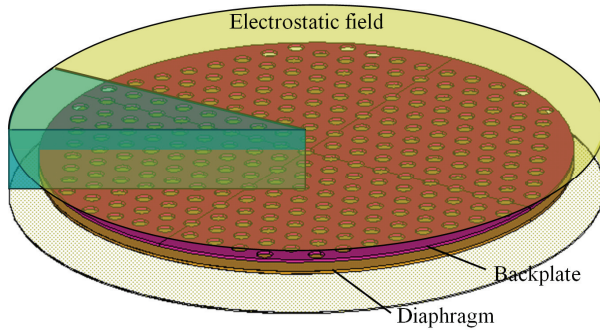
the diaphragm and backplate is  $2 \mu\text{m}$ . The voltage difference between them is 2 volts. Because the geometry is quite complicated, the triangulated surface boundary scheme was employed. Due to cyclic symmetry, it is sufficient to adopt one twelfth of the analysis domain for analysis as shown in Fig. 11(b). For the electrostatic field analysis, a moderate size of free space is included.

The ANSYS program is also employed to solve the same problem. The electric potential distribution is shown in Fig.11(c). With ANSYS, a convergence study was also conducted that the computed electric potentials at point y have converged to 0.621 Volts as shown in Table 2. The value obtained from the EFGM is 0.638 Volts within 3% difference. This example shows that even a very complicated analysis domain can be handled with the proposed scheme.

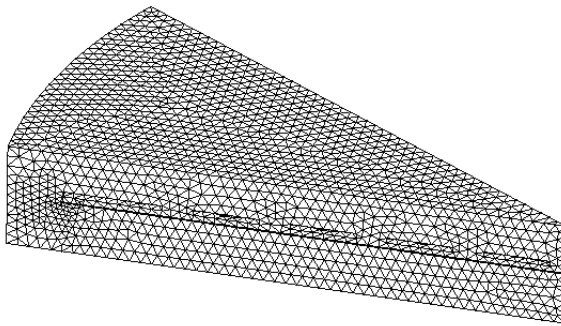
The third example is the analysis of the guinea pig's ossicles, i.e. the tiny bones of middle ear as shown in Fig. 2. They play the role of passing outside sound pressure to inner hearing nerves. Normally, the raw geometry data are obtained by CT (Computed tomography) scan from which a triangulated surface model is generated. Since the geometry is extremely irregular, the triangulated surface boundary scheme was used to calculate the stiffness of the ossicles, including the malleus, incus, and stapes. One end of the stapes is fixed and the other end of the malleus is loaded with  $18 \times 10^{-4}$  N force. The Young's modulus of bones is 14.1 Gpa, and Poisson's ratio is 0.3.

Table 2: Comparison of the computed electric potentials at point y

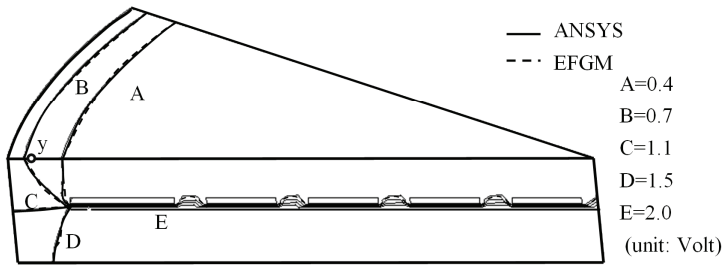
Method	No. of elements	No. of nodes	Electric potential (Volt)
ANSYS	3,795	3,901	0.601
	5,743	7,910	0.618
	16,235	35,602	0.622
	100,074	65,307	0.621
EFGM		19,618	0.638



(a) schematic diagram of a silicon microphone



(b) triangulated surface boundary scheme for a silicon microphone (1/12 model)



(c) electric potential distribution

Figure 11: Electrostatic analysis of a silicon microphone

Moreover, when certain part of ossicles is damaged or degraded due to some causes, e.g. ear infections, ossicular replacement prostheses may be employed to restore hearing function. The most popular material used is titanium, of which Young's modulus is 116 Gpa and Poisson's ratio is 0.32. When one or two of the ossicles are replaced with titanium material, this becomes a multi-material problem. In such situations, the present schemes and mechanisms established are still applicable. Each part, say, the malleus, incus and stapes, can be represented by a complete triangulated surface boundary domain and shares the adjacent triangulated interfaces with other parts as shown in Fig. 12.

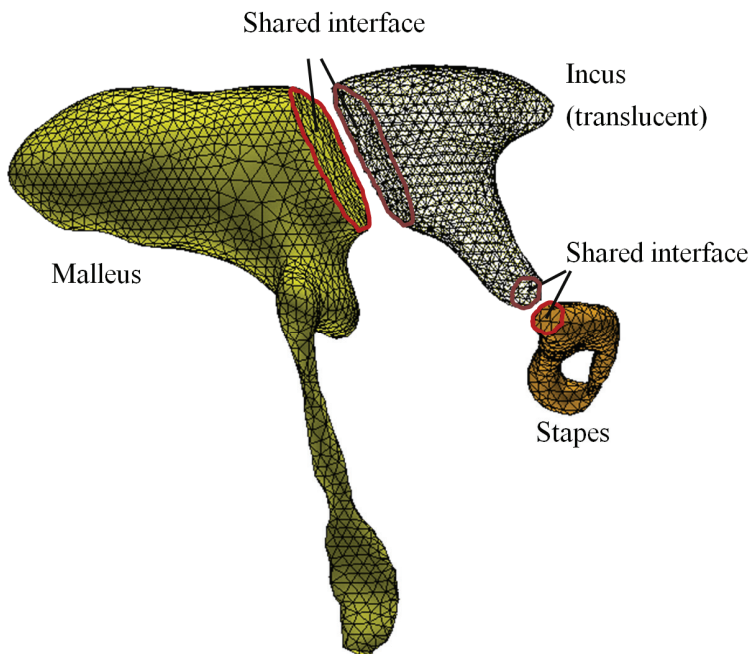


Figure 12: Multi-material model for guinea pig's ossicles

A comparison of the maximum displacement results of various cases is shown in Fig. 13. In case 1, all parts contained only the original bone material. In case 2, the stapes was replaced with titanium material. In case 3, the incus was replaced with titanium material. In case 4, the malleus was replaced with titanium material.

As would be expected, the finite element solutions with 25,414 4-node linear tetrahedral elements and 5,828 nodes were too stiff as compared to those with 25,414 10-node quadratic tetrahedral elements and 39,887 nodes. The results of the element-free Galerkin method with 2,889 nodes are quite consistent with the ANSYS's re-

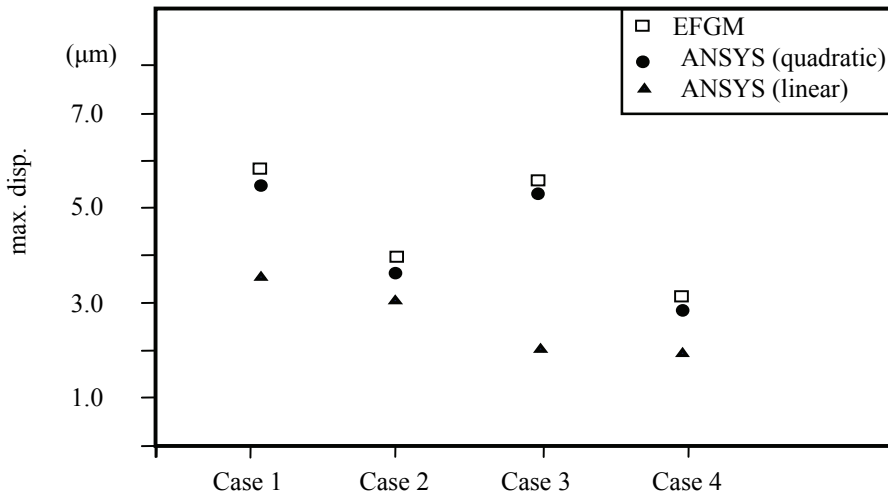


Figure 13: Comparison of max. displacement results

sults of the 10-node quadratic tetrahedral element model.

## 6 Conclusions

In this work, two types of geometry schemes, the constructive solid geometry scheme and the triangulated surface boundary scheme, have been proposed to define the three-dimensional analysis domain and its boundaries for the meshless method. The constructive solid geometry scheme is good for regular-shaped analysis domain which can be defined with basic primitives and appropriate set operations. Nevertheless, the triangulated surface boundary scheme is able to handle any kind of irregular geometry. Especially, following the displacements of the vertex nodes, the triangular facets can deform and move accordingly. This feature is needed for the continuously deformed nonlinear problems. In addition to the geometry representations, several efficient check mechanisms are also devised to solve some location issues needed for the meshless method. Using the same geometry schemes and check mechanisms, the multi-material problems, which are usually difficult to deal with by the meshless method, can also be effectively tackled. Several demonstrative cases prove the efficiency and advantages of the proposed schemes and mechanisms. In addition to the element free Galerkin method as adopted in this work, the proposed geometry schemes and check mechanisms are also applicable to other kinds of meshless methods, such as the meshless local Petrov-Galerkin method [Atluri and Zhu (1998)].

**Acknowledgement:** The authors would like to thank Dr. C.F. Lee of Taiwan Buddhist Tzu Chi General Hospital, and, Dr. C.M. Yao, Mr. L.C. Lee and Mr. L.M. Lee of the National Center for High-performance Computing in Taiwan for initiating the guinea pig's middle-ear study, the preparation of geometry data and valuable discussions. Part of the financial support came from the National Science Council, Taiwan, through grant NSC93-2212-E-007-017 is also acknowledged.

## References

- Atluri, S. N.; Zhu, T.** (1998): A new meshless local Petrov-Galerkin (MLPG) approach in computational mechanics. *Comput. Mech.*, Vol. 22, pp. 117–127.
- Atluri, S. N.; Han, Z. D. ; Rajendran, A. M.** (2004) : A New Implementation of the Meshless Finite Volume Method, Through the MLPG "Mixed" Approach, *CMES: Computer Modeling in Engineering & Sciences*, Vol. 6, no. 6, pp. 491-513.
- Belytschko, T.; Lu, Y.Y.; Gu, L.** (1994): Element-Free Galerkin Method. *International Journal for Numerical Methods in Engineering*, Vol. 37, pp. 229-256.
- Chen, W. H.; Guo, X. M.** (2001): Element Free Galerkin Method for Three-dimensional Structural Analysis, *CMES: Computer Modeling in Engineering & Sciences*, Vol. 2, no. 4, pp. 497-508.
- Chen, W. H.; Chen, C. H.** (2005): On Three-Dimensional Fracture Mechanics Analysis by an Enriched Meshless Method, *CMES: Computer Modeling in Engineering & Sciences*, Vol. 8, no. 3, pp. 177-190.
- Chen W.H.; Chi C.T.; Lee M.H.** (2009): A Novel Element-Free Galerkin Method with Uniform Background Grid for Extremely Deformed Problems, *CMES: Computer Modeling in Engineering & Sciences*, Vol.40, no.2, pp. 175-200.
- Duarte, C. A.; Oden, J. T.** (1996): An h-p adaptive method using clouds. *Computer Methods in Applied Mechanics and Engineering*, Vol. 139, pp.237-262.
- Han, Z. D.; Atluri, S. N.** (2004): Meshless Local Petrov-Galerkin (MLPG) approaches for solving 3D Problems in elasto-statics, *CMES: Computer Modeling in Engineering & Sciences*, Vol. 6, no. 2, pp. 169-188.
- Johnson, R. E.; Kiokemeister, F. L.; Wolk, E. S.** (1978): Calculus and Analytic Geometry, *William C Brown Pub.*
- Li, Q.; Shen, S.; Han, Z. D. ; Atluri, S. N.** (2003) : Application of Meshless Local Petrov-Galerkin (MLPG) to Problems with Singularities, and Material Discontinuities, in 3-D Elasticity, *CMES: Computer Modeling in Engineering & Sciences*, Vol. 4, no. 5, pp. 567-581.
- Liu, W. K., Jun, S. and Zhang, Y. F.** (1995) : Reproduction Kernel Particle meth-

ods, *International Journal for Numerical Methods in Fluids*, Vol. 20, pp. 1081-1106.

**Nagashima, T.** (2000): Development of a CAE system based on the node-by-node meshless method, *Computer Methods in Applied Mechanics and Engineering*, Vol. 187, pp.1-34.

**Zeid, I.** (1991): CAD/CAM Theory and Practice, *McGraw-Hill Inc.*

